Effect of hydrogen and thermal aging on plastic deformation of a duplex stainless steel

Rana Bchara, Ingrid Proriol Serre, Jean-Bernard Vogt

EFFECT OF HYDROGEN AND THERMAL AGING ON PLASTIC DEFORMATION OF A DUPLEX STAINLESS STEEL

[1]Rana BCHARA, [1]Ingrid PRORIOL SERRE, [1]Jean-Bernard VOGT

[1]University of Lille, CNRS, INRAE, Centrale Lille, UMR 8207 - UMET - Unité Matériaux et Transformations, Lille, France, EU, rana.bchara.etu@univ-lille.fr

https://doi.org/10.37904/metal.2022.4405

Abstract

In this paper, the effects of hydrogen charging and aging treatment on the cyclic plasticity of a S32304 lean duplex steel were investigated. The surface modifications were analyzed using atomic force microscopy and scanning electron microscopy. The slip morphologies of annealed, hydrogenated or thermally aged specimens were compared after cyclic loading at $\Delta\varepsilon_p$= 0.07%. Significant changes were detected for austenite charged with hydrogen and for ferrite thermally aged. The results indicated a planar slip mode with a secondary slip for hydrogenated austenite. The height and the spacing between the slip marks of austenite (SBH and SBS) decreased from [30-5] nm to [8-2] nm and from [3-0.7] μm to [1-0.2] μm respectively with hydrogen addition. The morphology and the mean value of SBH and SBS of ferrite slip lines remained the same after 5 h of hydrogen charging. However, the increase of hydrogen charging duration created micro-cracks inside the slip bands of ferrite and decreased the value of their SBH and SBS. The thermally aged steel developed straight slip bands inside the ferrite after cyclic loading while they were curvilinear in the annealed material. The effect of the α-phase spinodal decomposition was pointed out even for a short aging duration.

Keywords: AFM, Plastic deformation, Stainless steel, Fatigue slip marks

1. INTRODUCTION

Duplex stainless steels (DSS) are known for their good corrosion resistance and mechanical properties. This excellent combination allowed DSS to be widely used in many industries such as petrochemical, nuclear, oil and gas transportation [1]. However, in these environments, the applications of DSS can be limited due to hydrogen embrittlement (HE) and 475 °C embrittlement [2].

The presence of two phases, austenite (γ) and ferrite (α), inside DSS complicates the understanding of the effect of hydrogen on its mechanical behavior. Austenite presents a face centered cubic structure (FCC) which allows a high hydrogen solubility, while ferrite exhibits a body centered cubic structure (BCC) that enables a high hydrogen diffusivity but a low solubility [1]. Moreover, hydrogen embrittlement occurrence depends on the metallurgical state of the material (aged, cold worked), e.g. [1-3].

An important effect of hydrogen on the degradation of the steel is the presence of cracks on the surface due to a local accumulation of hydrogen [4,5]. In addition, a martensitic transformation (ε or α'-martensite) can occur in austenite during the hydrogen charging possibly promoted by straining [1,6]. For instance, Okayasu et al. [3] showed a severe HE of DSS due to various hydrogen trapping sites and its high diffusivity. They noticed a ductility loss of the material while increasing the hydrogen charging. Therefore, to comprehend the hydrogen embrittlement of DSS it is important to study its effect on the plasticity of each phase of the steel.

Besides hydrogen embrittlement, aging DSS at 475 °C can be deleterious for their ductility and can even embrittle the steel. Most of the studies [7-9] have investigated the embrittlement of DSS after a long aging time. It affects the ferrite phase which decomposes into Fe-rich α' and Cr-rich α'' at 475 °C by a spinodal

decomposition. Ferrite shows a complex interconnected structure between α' and α'' that can lower the mobility of dislocations and even promotes twinning. According to some studies, the spinodal decomposition in DSS is triggered after an aging treatment for a short time [10,11] without any brittleness.

The objective of the present paper is to investigate how the presence of hydrogen and a short time 475 °C aging can affect the plasticity response of each phase of a DSS. To obtain rather large plastic strain without instability or fracture, the investigated materials were subjected to cyclic plastic deformation in order to accumulate plastic strain.

2. MATERIAL AND METHODOLOGY

The lean duplex stainless steel (LDSS) used in this study has been provided by Aperam company. The steel has been supplied as annealed and pickled sheets with 5 mm as final thickness. Its chemical composition is given in **Table 1** which according to ASTM corresponds to the S32304 grade.

Table 1 Chemical composition of the studied S32304 DSS in wt%

Chemical elements	Cr	Ni	Mn	Mo	Si	N	C	Fe
wt%	22.71	3.85	1.79	0.47	0.45	0.125	0.018	Bal.

The microstructure of the LDSS was observed using optical microscopy after etching with Beraha reagent (solution of 4g NH_4HF_2, 1g $K_2S_2O_5$, 80 mL H_2O and 40 mL HCl) for 10 s. **Figure 1** shows the micrograph taken along the rolling direction where the dark phase corresponds to α-ferrite and the bright one to γ-austenite.

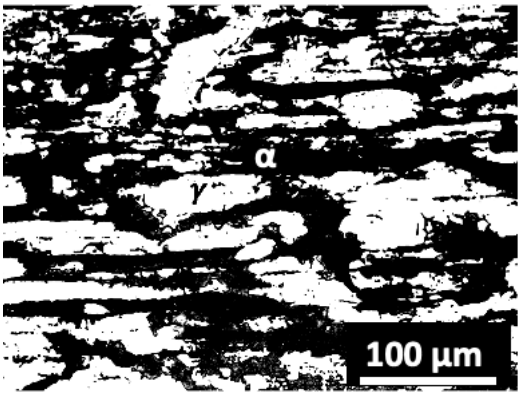

Figure 1 Optical micrograph of the S32304 LDSS showing ferrite (α) and austenite (γ)

Three microstructural states were investigated: annealed, cathodically hydrogen charged and thermally aged at 475 °C. To acquire large plastic strain, low cycle fatigue (LCF) test has been carried out on flat specimen extracted along the rolling direction of the plate. The specimens had a gauge length of 12 mm, and a cross-section of 6 x 0.5 mm^2. Samples were prepared first by mechanical polishing with final 1 µm diamond paste. Then, they were electro-polished in a solution of 80% acetic acid, 10% perchloric acid and 10% of distilled water at 25 V. Fatigue tests were performed under controlled total strain during 1500 cycles in order to obtain a plastic strain variation equal to $\Delta\varepsilon_p$ = 0.07 % at each cycle.

Hydrogen was introduced into the steel by using an electrochemical cell at a cathodic current density of 10 mA/cm^2 in a 0.5M H_2SO_4 electrolyte containing 0.2 g/L As_2O_3 to prevent the combination of hydrogen. The charging was performed at room temperature for 5 h and 24 h on polished samples as mentioned before then subjected to LCF tests.

For the aging treatment, a sample was heated in a muffle furnace at 475 °C for 25 h and then cooled at room temperature. The surface preparation was performed after the aging treatment and before the cycling test.

Atomic force microscopy (AFM) analyses were carried out on deformed samples to characterize their slip marks patterns. The analyses were conducted in tapping mode using Veeco Nanoscope III AFM. The topographic mode was used for the measurement of the heights of the slip bands (SBH) and the spacing between the slip bands (SBS). Additionally, Scanning Electron Microscopy (SEM) analyses were performed on the surface of each sample.

3. RESULTS AND DISCUSSION

3.1. Slip marks pattern in the annealed LDSS

Plasticity marks were observed on the surface of both phases after loading the annealed specimen. The slip marks or slip bands were more or less developed being therefore labelled as slip steps or as fatigue extrusions. The slip bands were straight and inclined with the loading axis in austenite (**Figure 2 a)** while they were curvilinear in the ferrite. The morphology of the slip bands in austenite suggests that the dislocation slip mode should be planar.

3.2. Slip marks patterns in the LDSS microstructure after hydrogen charging

After 5 and 24 hours of hydrogen charging of LDSS (LDSS-5H, LDSS-24H), the austenite was mostly covered by slip steps instead of extrusions. Moreover, activation of a second slip system of the austenite was more frequently observed, as illustrated in **Figure 2 b**. The smoothness of the slip lines is well defined after the hydrogen addition. SBH and SBS in the austenite grains decrease from [30-5] nm to [8-2] nm and from [3-0.7] to [1-0.2] μm respectively after 5 h and 24 h of charging. The slip planarity appears to be more marked in agreement with literature results [12,13] which can be related to a reduction of stacking fault energy induced by hydrogen. Restricted cross-slip and less developed slip bands suggest that hydrogen restricts mobility of dislocations which imply more austenite grains to accommodate the plasticity.

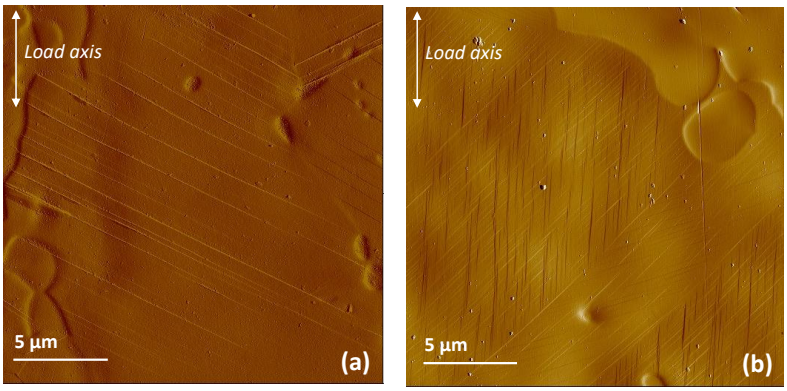

Figure 2 AFM amplitude signal error images of slip marks in austenite, (a): for annealed LDSS; (b): for LDSS-5H

No significant change was observed in ferrite grains after 5 h of hydrogen charging.

However, the hydrogen charging for 24 h affects the relief in ferrite. SBH decrease from [30-15] nm to [18-5] nm and others [8-4] nm likewise SBS decrease from [0.9-3] μm to [0.5-1] μm. The slip bands in ferrite were narrower and occasionally accompanied by micro-cracks in the hydrogenated LDSS after 24h in comparison with the annealed one (**Figure 3**). Hence, the hydrogen concentration provided from 5 hours of charging seems to be insufficient to generate modifications in ferrite phase and therefore trapped in austenite. These results

indicate that austenite is the first hydrogen trapping site. The increase of hydrogen charging duration leads to a hydrogen saturation of both phases.

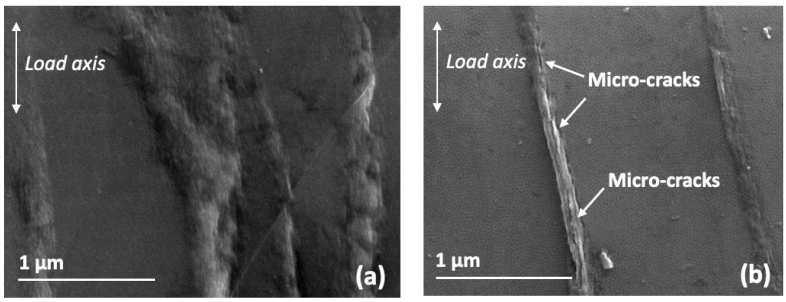

Figure 3 SEM images of ferrite (a): for annealed LDSS; (b): for LDSS-24H showing the presence of the micro-cracks associated to the slip band

3.3. Effect of 475 °C aging

After aging at 475 °C for 25 hours (LDSS- 475 °C), the microhardness of ferrite increased from $Hv_{0.25}$ = 236±5 to $Hv_{0.25}$ = 270±6 while no variation in microhardness was noted for austenite ($Hv_{0.25}$ = 259±7), confirming thus an effect of the aging treatment even for a short duration [14]. Similar results were obtained by Reis et al. [10] on the same LDSS. They pointed out the occurrence of the spinodal decomposition inside the ferrite by the change of the height values between ferrite and austenite phases of chemically etched surfaces using scanning probe microscopy analyses operating in AFM. They noticed a significant height decrease after 25 hours of aging then the height value remains almost the same while increasing the aging treatment duration.

To point out the effect of the 25 h - 475 °C aging treatment, hysteresis loops recorded during cycling the annealed and aged specimens were analyzed with the aim to assess the effective stress, the short distance interactions thermal stress. For that, the Handfield-Dickson's method has been used. It consists in a graphical treatment of the loop where the effective stress is determined using the two frontiers (σ_{emax} et σ_{emin}) in regards to the elastic line as shown in **Figure 4.**

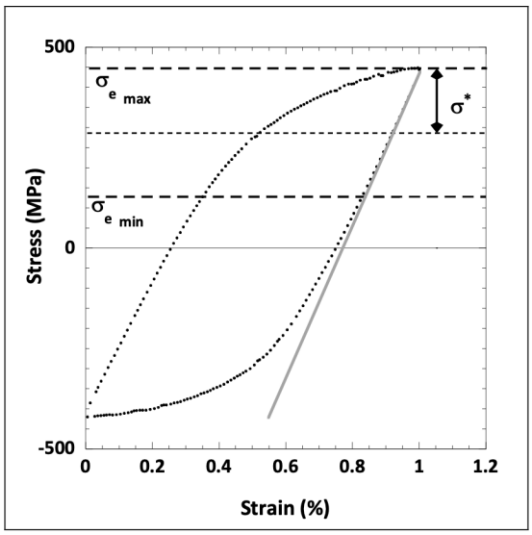

Figure 4 Assessment of the effective stress from an hysteresis loop

The effective stress (σ^*) is calculated using equation (1):

$$\sigma* = \frac{\sigma_{emax} - \sigma_{emin}}{2} \quad (1)$$

Where:

$\sigma*$ - the effective stress (MPa)

σ_{emax} - the maximum stress (MPa)

σ_{emin} - the minimum stress (MPa)

While the annealed LDSS material exhibits an effective stress (σ*) value of 235 MPa during the first cycle of fatigue, the latter grows up to 320 MPa for the aged LDSS - 475 °C. Then with the following cycles, the effective stress considerably vanishes for the aged LDSS - 475 °C material to remain at an average value of 150 MPa, lower than that of the LDSS annealed material (**Figure 5**). Regarding summarization, the aging leads to an increase in the effective stress (σ*) of the LDSS material together with an increase in hardness only in ferrite and not in austenite. It can be therefore concluded that 25 h is indeed enough to modify the microstructure of the ferrite in the S32304 LDSS and influences the dislocation displacements. At first, the aging is suspected to redistribute atoms such as chromium which may anchor the dislocations enough to require a stress overflow to obtain plasticity. Then, once dislocations are unanchored, they can move easily in "clean" tracks between the clusters of chromium resulted from the segregation in the α-phase. This has also been confirmed by the straight shape of slip bands in ferrite observed by AFM after the aging treatment.

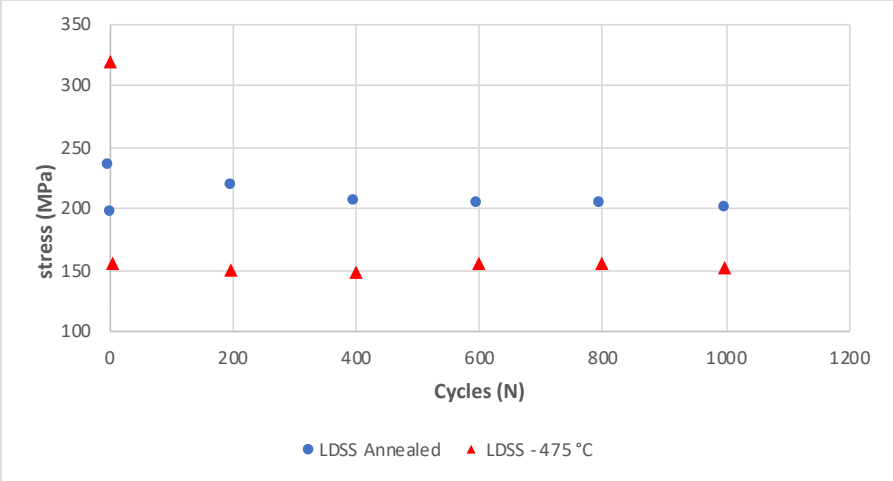

Figure 5 Evolution of the effective stress of annealed and aged duplex versus the number of cycles

4. CONCLUSION

This paper has highlighted the importance of the metallurgical state - annealed, hydrogen enriched or thermally aged - on the plastic deformation of each phase of a lean duplex stainless steel S32304. The topographic modifications produced by cyclic loading were detected by using AFM and SEM for the three different states of the steel. The main results are summarized as follows:

- Slip bands were less high and less spaced inside the austenite grains after hydrogen addition.
- The slip bands morphology in austenite suggested a planar slip mode enhanced by the presence of hydrogen.
- Hydrogen hinders dislocation mobility in austenite which makes additional austenite grains to be active.
- No clear change was identified for ferrite grains after 5 hours of hydrogen charging.
- Hydrogen charging for 24 hours induced the presence of micro-cracks inside the ferrite slip bands.
- A significant hardening of ferrite was obtained after 25 hours of aging treatment (475 ˚C), reason of the spinodal decomposition inside the ferrite, while the behavior of austenite remains unchanged.
- Ferrite of thermally aged LDSS developed straight slip bands.

ACKNOWLEDGEMENTS

For their participation to this study, the authors thank D. Creton and J. Golek. Observations by SEM were performed at the electron microscope facility at Lille University with the support of Chevreul Institute, the European Regional Development Fund, and the Region Hauts-de-France (France).

REFERENCES

[1] L. CLAEYS, I. DE GRAEVE, T. DEPOVER, AND K. VERBEKEN. Hydrogen-assisted cracking in 2205 duplex stainless steel: Initiation, propagation and interaction with deformation-induced martensite. *Mater. Sci. Eng. A*. [online]. 2020, vol. 797, p. 140079. Available from: https://doi.org/10.1016/j.msea.2020.140079.

[2] J. WOODTLI and R. KIESELBACH. Damage due to hydrogen embrittlement and stress corrosion cracking. *Eng. Fail. Anal.* [online]. Dec. 2000, vol. 7, no. 6, pp. 427-450. Available from: https://doi.org/10.1016/S1350-6307(99)00033-3.

[3] M. OKAYASU and T. FUJIWARA. Effects of microstructural characteristics on the hydrogen embrittlement characteristics of austenitic, ferritic, and γ-α duplex stainless steels. *Mater. Sci. Eng. A*. [online]. Mar. 2021, vol. 807, p. 140851. Available from: https://doi.org/10.1016/j.msea.2021.140851.

[4] K. O. FINDLEY, M. K. O'BRIEN, and H. NAKO. Critical Assessment 17: Mechanisms of hydrogen induced cracking in pipeline steels. *Mater. Sci. Technol.* [online]. Nov. 2015, vol. 31, no. 14, pp. 1673-1680. Available from: https://doi.org/10.1080/02670836.2015.1121017.

[5] V. VENEGAS, F. CALEYO, J. L. GONZÁLEZ, T. BAUDIN, J. M. HALLEN, and R. PENELLE. EBSD study of hydrogen-induced cracking in API-5L-X46 pipeline steel. *Scr. Mater.* [online]. Jan. 2005, vol. 52, no. 2, pp. 147-152. Available from: https://doi.org/10.1016/j.scriptamat.2004.09.015.

[6] M. BREDA, K. BRUNELLI, F. GRAZZI, A. SCHERILLO, and I. CALLIARI. Effects of Cold Rolling and Strain-Induced Martensite Formation in a SAF 2205 Duplex Stainless Steel. *Metall. Mater. Trans. A*. [online]. Feb. 2015, vol. 46, no. 2, pp. 577-586. Available from: https://doi.org/10.1007/s11661-014-2646-x.

[7] C. ÖRNEK, M. BURKE, T. HASHIMOTO, and D. ENGELBERG. 748 K (475 °C) Embrittlement of Duplex Stainless Steel: Effect on Microstructure and Fracture Behavior. *Metall. Mater. Trans. A*. [online]. Jan. 2017, vol. 48. Available from: https://doi.org/10.1007/s11661-016-3944-2.

[8] R. SILVA, C. A. DELLA ROVERE, and S. E. KURI. Effect of Thermal Aging at Low Temperature on the Mechanical Properties and Corrosion Resistance of LDX 2404 Duplex Stainless Steel. *Mater. Sci. Forum*. [online]. 2016, vol. 869, pp. 705-710. Available from: https://doi.org/10.4028/www.scientific.net/MSF.869.705.

[9] S. C. SCHWARM, S. MBURU, R. P. KOLLI, D. E. PEREA, and S. ANKEM. Effects of long-term thermal aging on bulk and local mechanical behavior of ferritic-austenitic duplex stainless steels. *Mater. Sci. Eng. A*. [online]. Mar. 2018, vol. 720, pp. 130-139. Available from: https://doi.org/10.1016/j.msea.2018.02.058.

[10] T. J. ÁVILA REIS, H. M. SANTOS, E. W. REIS DE ALMEIDA, and L. B. GODEFROID. Microstructure evolution and mechanical behavior of a lean duplex stainless steel aged at 475Oc. *Mater. Sci. Eng. A*. [online]. Apr. 2021, vol. 810, p. 141028. Available from: https://doi.org/10.1016/j.msea.2021.141028.

[11] S. S. M. TAVARES, J.M. PARDAL, H. FERREIRA GOMES DE ABREU, C. DOS SANTOS NUNES, and M. RIBEIRO DA SILVA. Tensile Properties of Duplex UNS S32205 and Lean Duplex UNS S32304 Steels and the Influence of Short Duration 475 °C Aging. *Mater. Res.* [online]. 2012, vol. 15, pp. 859-864. Available from: https://doi.org/10.1590/S1516-14392012005000116.

[12] A. E. PONTINI and J. D. HERMIDA. "X-Ray diffraction measurement of the stacking fault energy reduction induced by hydrogen in an AISI 304 steel." *Scr. Mater.* [online]. Dec. 1997, vol. 37, no. 11, pp. 1831-1837. Available from: https://doi.org/10.1016/S1359-6462(97)00332-1.

[13] M. MÉNARD, J. M. OLIVE, A.-M. BRASS, and I. AUBERT, "Effects of hydrogen charging on surface slip band morphology of a type 316L stainless steel." in *Environment-Induced Cracking of Materials*, S. A. [online]. SHIPILOV, R. H. JONES, J.-M. OLIVE, and R. B. REBAK, Eds. Amsterdam: Elsevier, 2008, pp. 179-188. Available from: https://doi.org/10.1016/B978-008044635-6.50017-0.

[14] K. CHANDRA, V. KAIN, V. BHUTANI, V.S. RAJA, R. TEWARI, G.K. DEY and J.K. CHAKRAVARTTY. Low temperature thermal aging of austenitic stainless steel welds: Kinetics and effects on mechanical properties. *Mater. Sci. Eng. A*. [online]. Feb. 2012, vol. 534, pp. 163-175. Available from: https://doi.org/10.1016/j.msea.2011.11.055.